Unveiling the Key Role of Aggregation in the Self-Doping of Conjugated Polyelectrolytes

Fernando Muñoz-Alba[a,b], Lorenzo Soprani[c], Benedetta Maria Squeo[d], Mariacecilia Pasini[d], Raúl González-Núñez[a,b], Rocío Ponce Ortiz[a,b], M. Carmen Ruiz Delgado[a,b*], Luca Muccioli[c*], Barbara Vercelli[e*]

[a]Departamento de Química Física, Universidad de Málaga, Málaga ES-29071 (Spain)

[b]Instituto Universitario de Materiales y Nanotecnología, IMANA, University of Malaga, 29071 Malaga (Spain)

[c]Dipartimento di Chimica "Toso Molinari", Università di Bologna, Bologna I-40136 (Italy)

[d]Istituto di Scienze e Tecnologie Chimiche "Giulio Natta" SCITEC-CNR, Via Corti 12, Milano I-20133 (Italy)

[e]Istituto di Chimica della Materia Condensata e di Tecnologie per l'Energia ICMATE-CNR, Via Cozzi 53, Milano I-20125 (Italy)

1. Synthesis

Materials - All used chemicals and solvents were reagent grade and used as received.

General Information for synthesis. All glassware was oven dried. Unless specifically mentioned, all chemicals are commercially available and were used as received. The dialysis membrane (MWCO: 3500–5000 Da) was purchased from Membrane Filtration Products Inc.

Polymers CPE-K and CPE-2K. Polymers **CPE-K** and **CPE-2K** were synthetized according to our procedure reported in ref. https://doi.org/10.3390/molecules26030763.

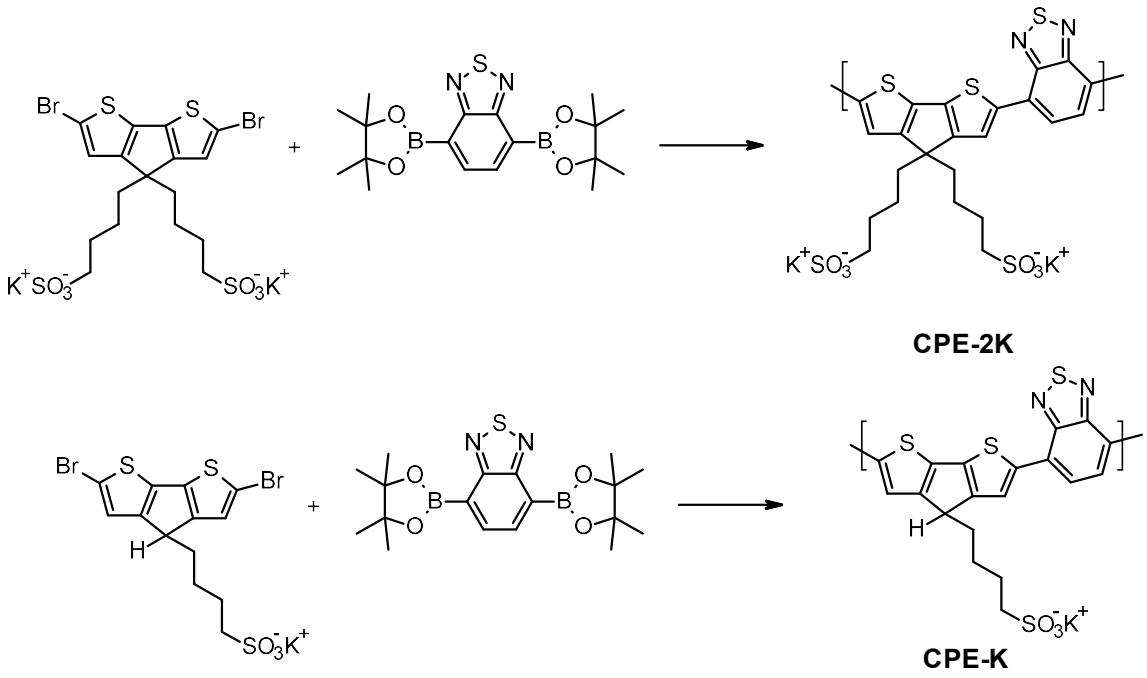

Scheme 1. Schematic synthesis of the polymers.

2. UV-VIS

Sample	H_2O	$EtOH/H_2O$	DMF/H_2O	$DMSO/H_2O$	DMF
CPE-2K	1.42	0.28	0.14	0.10	0
CPE-K	0.46	0.46	0.30	0.26	0

Table S1 - Relative intensity ratio ($A_{polaron}/A_{ICT}$) for **CPE-2K** and **CPE-K** at 0.025 mg·mL^{-1} in different solvents. Ratios were obtained by dividing the intensity of each band at its λ_{max} after subtracting the DMF baseline, where the polaron band is absent.

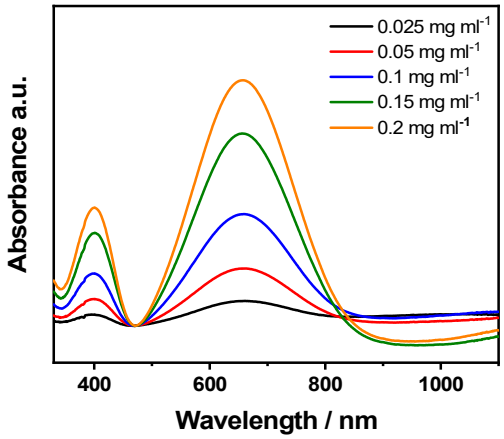

Figure S1. UV-vis spectra in water of **CPE-K** in the concentration range 0.025-0.2 mg mL^{-1}.

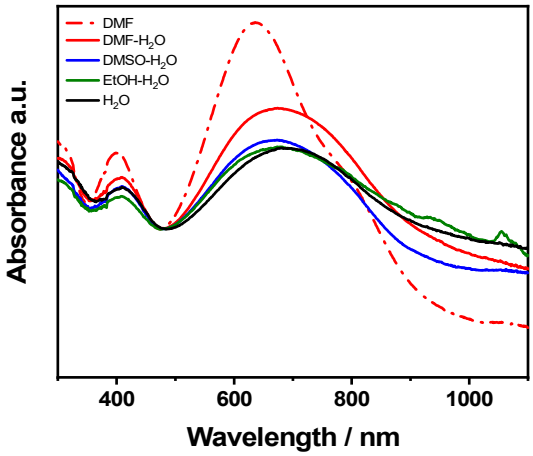

Figure S2. UV-vis spectra in water of **CPE-K** 0.025 mg mL^{-1} in different solvents.

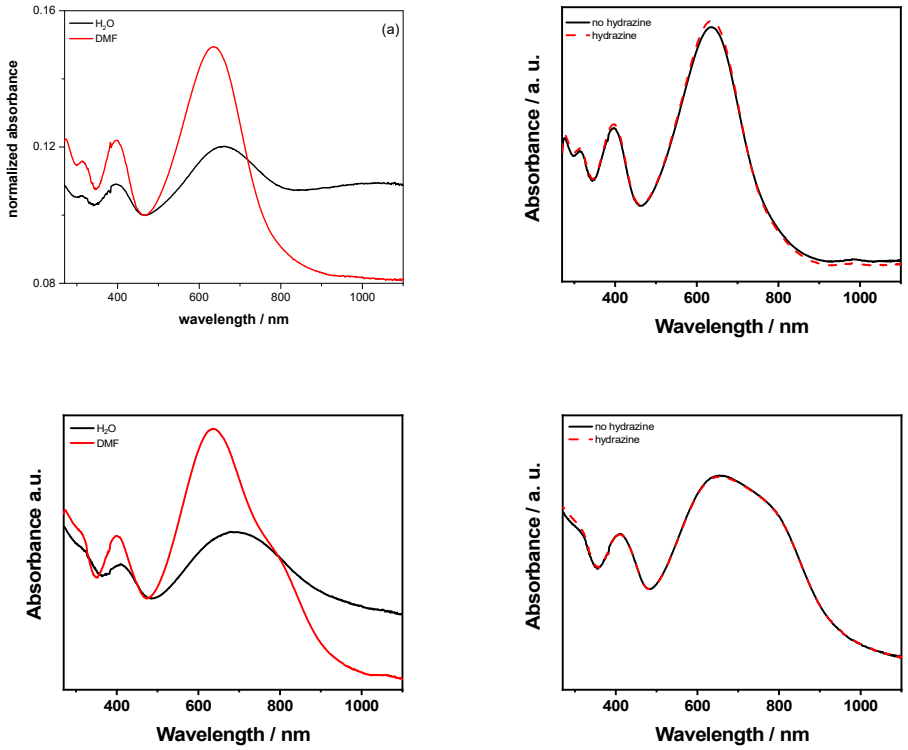

Figure S3. UV-vis spectra in water and DMF of (a) **CPE-2K** and (c) **CPE-K**. UV-vis spectra in DMF before and after hydrazine addition of (c) **CPE-2K** and (d) **CPE-K**.

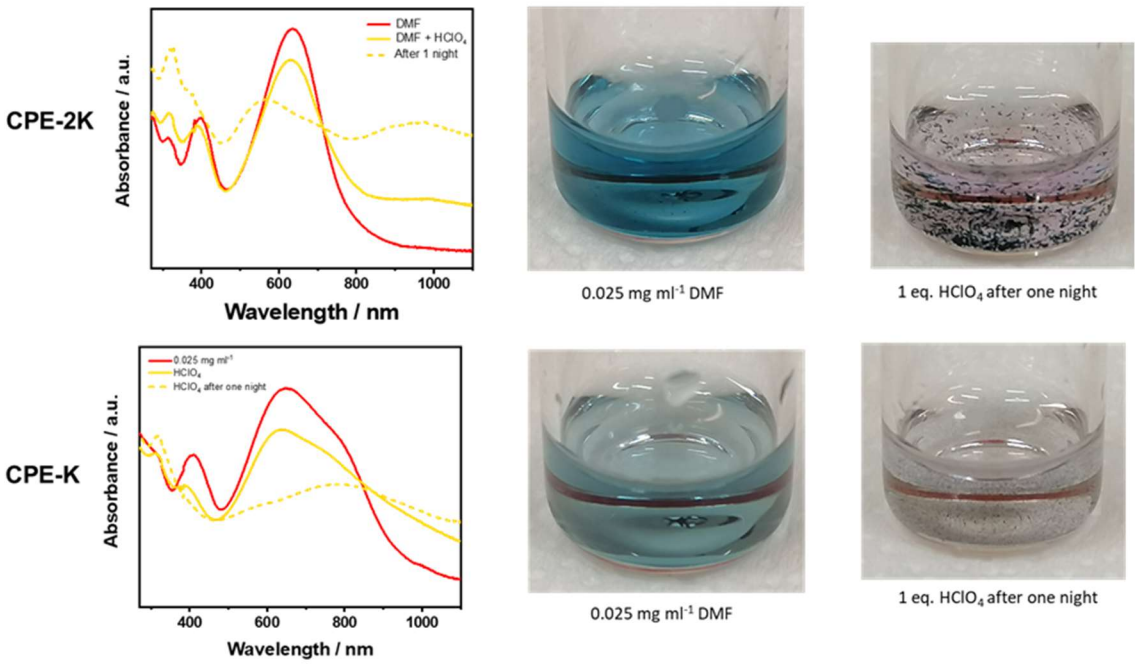

Figure S4. UV-vis spectra of **CPE-2K** and **CPE-K** 0.025 mg mL^{-1} in DMF before (red line), adding of 1 eq. of $HClO_4$ (orange line) and after 1 night (orange dashed line) and photographs of **CPE-2K** 0.025 mg mL^{-1} in DMF with 1 eq. $HClO_4$.

3. Theoretical calculations

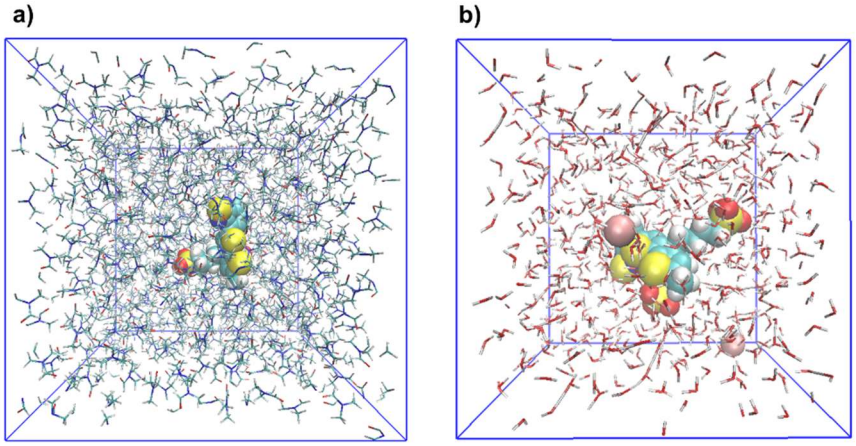

Figure S5. Simulation box of **CPE-2K** monomer in DMF (a) and water (b).

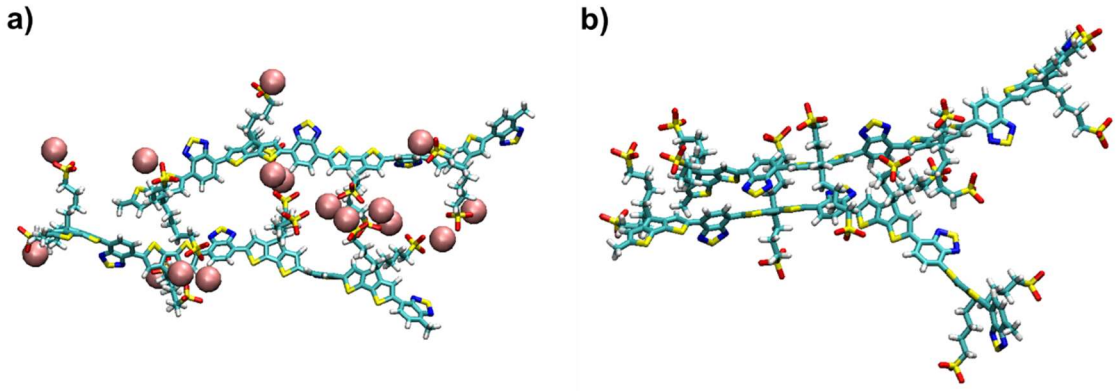

Figure S6. MD snapshot of **CPE-2K** tetramers in water (a) and DMF (b).

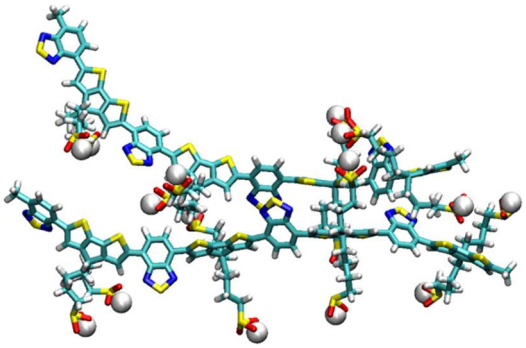

Figure S7. MD snapshot of **CPE-2K** tetramers in DMF including protons.

Sample	H_2O	NaOH	TBAOH
CPE-2K	1.02	0.84	0.80
CPE-K	0.85	0.83	0.65

Table S2. Ratio between polaron and ICT peaks $A_{polaron}/A_{ICT}$, calculated from the experimental spectra of **CPE-K** and **CPE-2K** polymers in pure water and after the addition of one equivalent of NaOH or TBAOH, respectively.

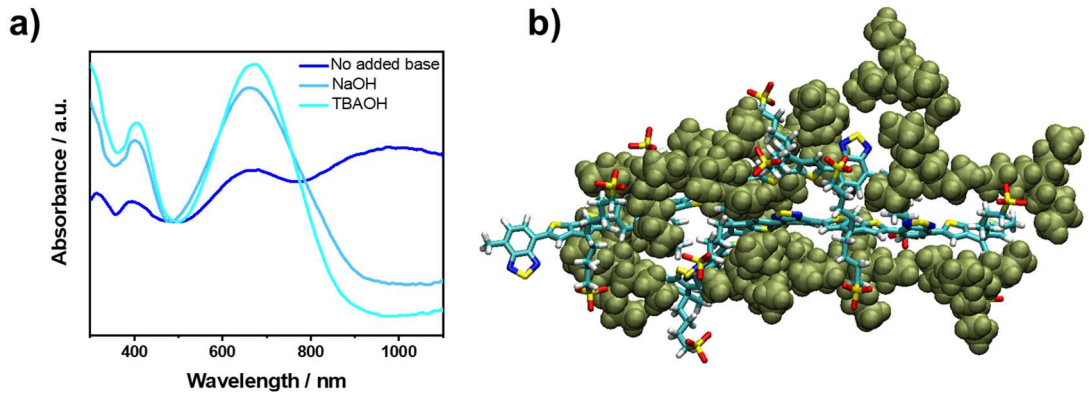

Figure S8. UV-VIS spectra of **CPE-2K** in pure water and after the addition of one equivalent of NaOH or TBAOH, respectively (a). MD snapshot of CPE-2K showing TBA^+ in green (b).

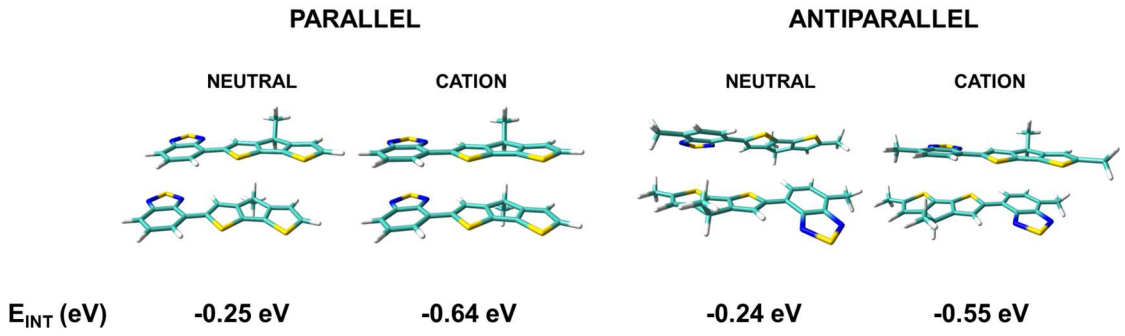

Figure S9. PBE0-D3/6-31G** interaction energies for the neutral and radical cation parallel and antiparallel **CPE-K** dimer models.

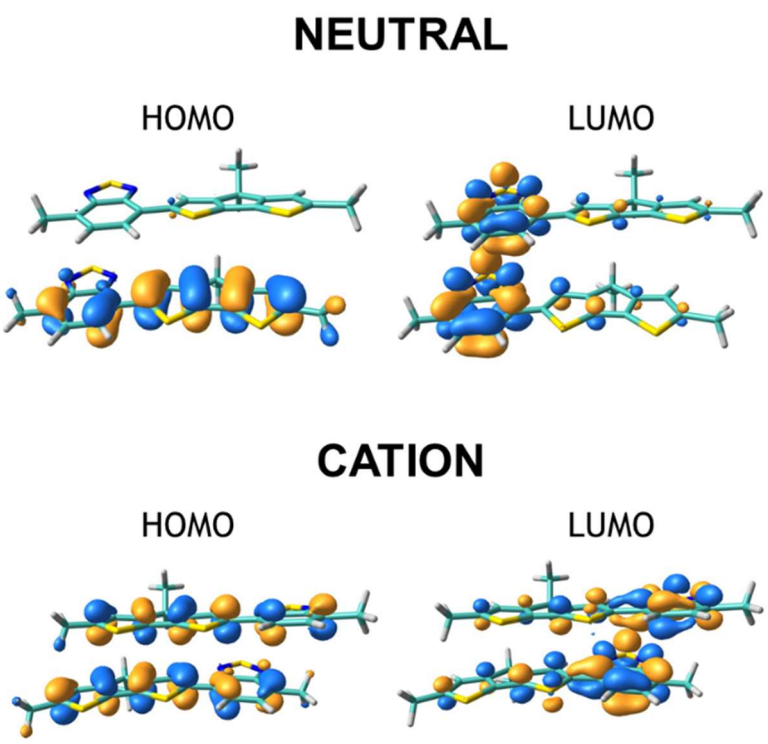

Figure S10. Frontier molecular orbitals (PBE0-D3/6-31G**) of the parallel neutral and radical cation **CPE-K** dimer models.

4. Raman Spectroscopy

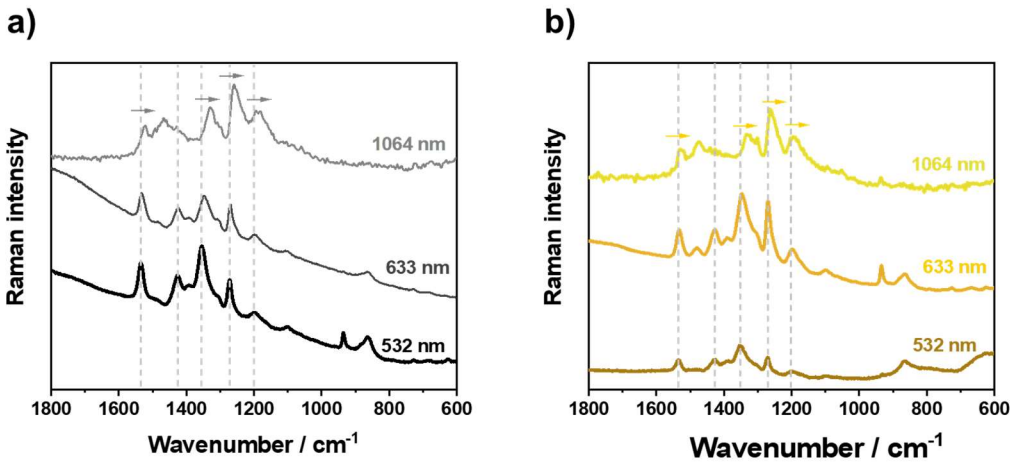

Figure S11. Solid state Raman spectra of **CPE-2K** (a) and **CPE-K** proton-aggregated form in DMF (b) at different excitation wavelengths.

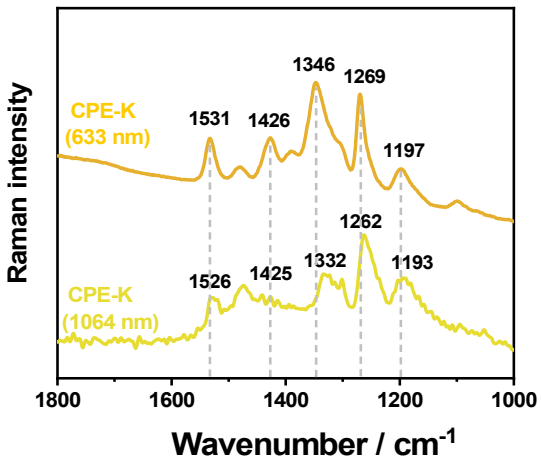

Figure S12. Raman spectra of the proton-aggregated form in DMF of **CPE-2K** upon excitation at 633 and 1064 nm.

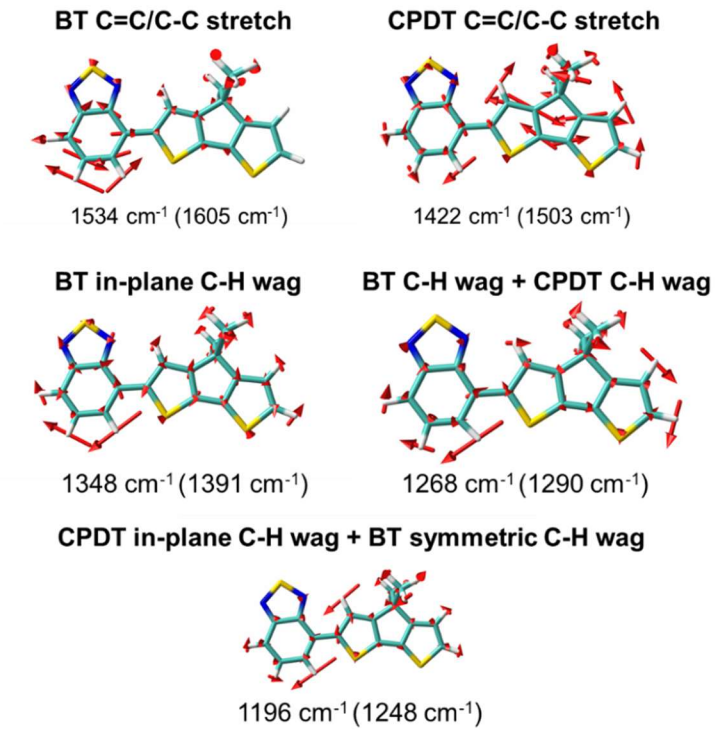

Figure S13. PBE0/6-31G** vibrational eigenvectors associated with the most outstanding Raman features of **CPE-2K** in neutral state. The measured and theoretical (in parentheses) wavenumbers are also given.

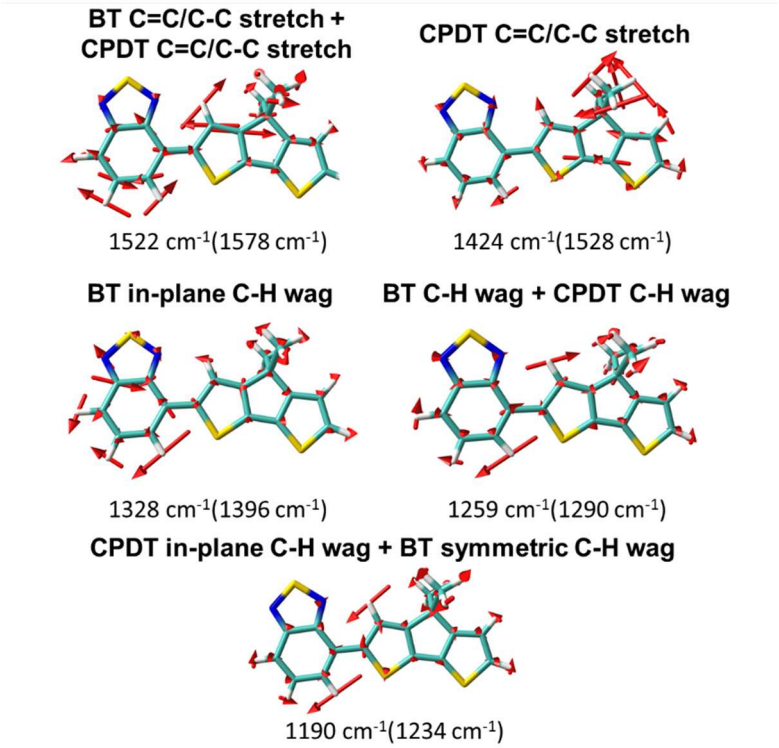

Figure S14. PBE0/6-31G** vibrational eigenvectors associated with the most outstanding Raman features of **CPE-2K** in cation state. The measured and theoretical (in parentheses) wavenumbers are also given.

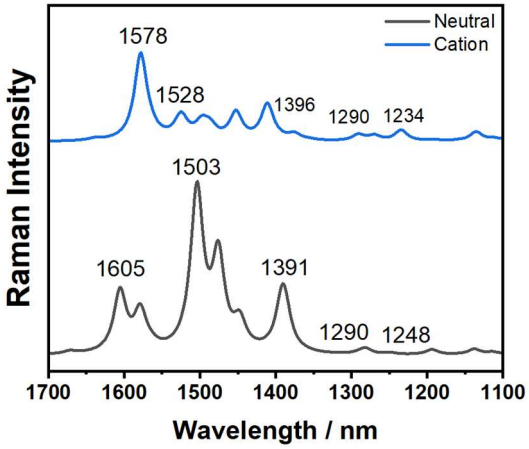

Figure S15. Theoretical (PBE0/6-31G**) Raman spectra for **CPE-2K** in neutral and radical cation state.

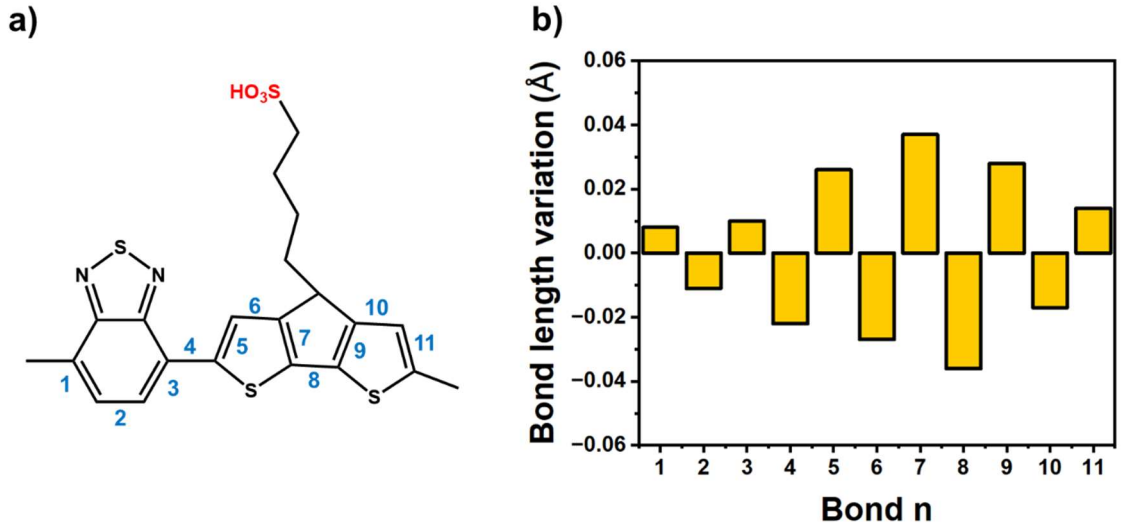

Figure S16. Bond assignation (a) and PBE0/6-31G** calculated bond length variation from the neutral monomer to the radical cation (b)

5. Cyclic Voltammetry

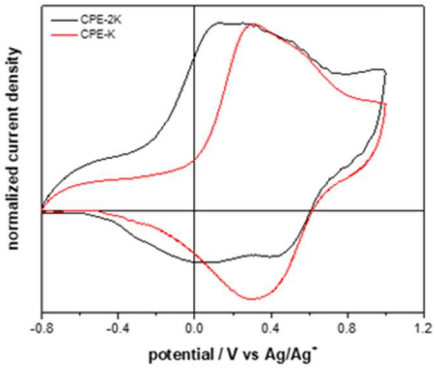

Sample	E^0_{ox}/ V
CPE-2K	0.0976; 0.33
CPE-K	0.28; 0.44

Figure S17. Cyclic Voltammograms of **CPE-2K** and **CPE-K** thin films cast from H_2O on GC electrode. Solvent: AN + 0.1 M TBAP. Scan rate: 0.1 Vs^{-1} and reversible oxidation potentials (E^0_{ox}) of **CPE-2K** and **CPE-K**.

System	Average Stacking lifetime	Average Angle between Stacked units
CPE-2K	2646	37
CPE-K	3463	33

Table S3. Additional stacking parameters averaged from 10 MD simulations with 2 tetramers of **CPE-K and CPE-2K** in water with randomized starting geometries.

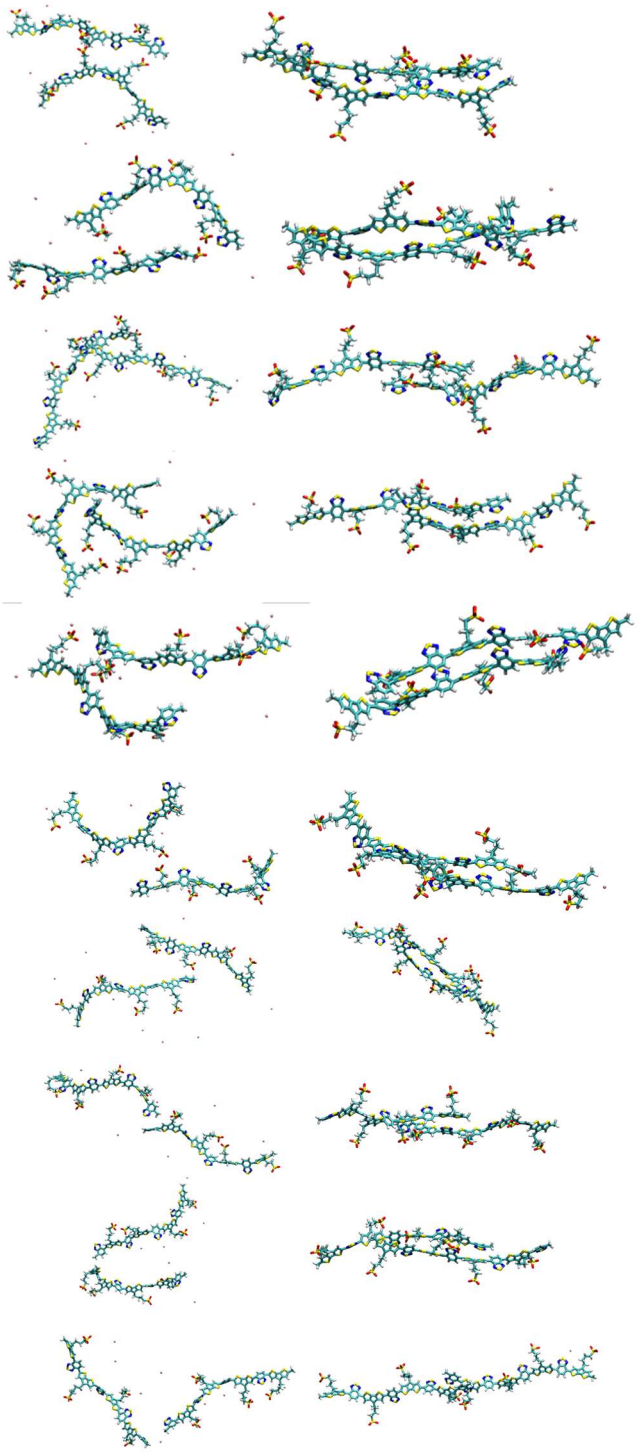

Figure S18. MD snapshots of CPE-K simulations in water with random starting geometries (left) and the last snapshot of the equilibrium phase (right).

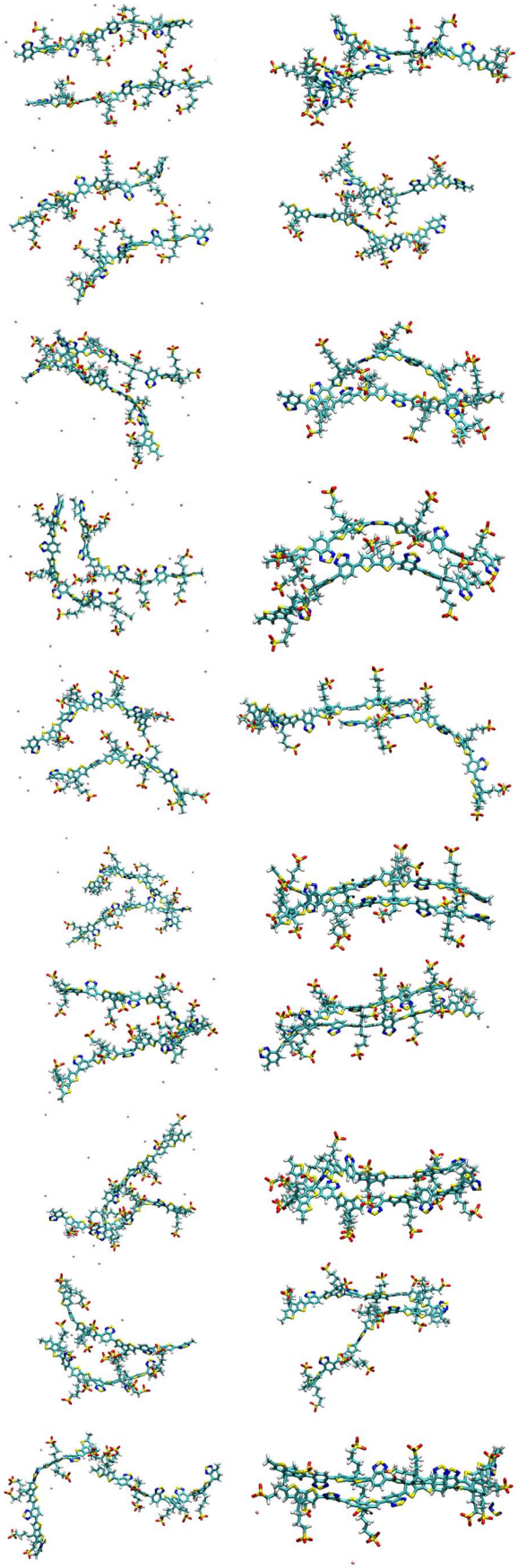

Figure S19. MD snapshots of CPE-2K simulations in water with random starting geometries (left) and the last snapshot of the equilibrium phase (right).